

# Bivalent Ligands Derived from Huperzine A as Acetylcholinesterase Inhibitors

H. Haviv<sup>1</sup>, D.M. Wong<sup>2</sup>, I. Silman<sup>3</sup> and J.L. Sussman<sup>4,\*</sup>

<sup>1</sup>Department of Biological Chemistry, Weizmann Institute of Science, Rehovot 76100, Israel, <sup>2</sup>Department of Chemistry, Virginia Tech, Blacksburg, VA 24061, USA, <sup>3</sup>Department of Structural Biology, Weizmann Institute of Science, Rehovot 76100, Israel, <sup>4</sup>Department of Neurobiology, Weizmann Institute of Science, Rehovot 76100, Israel

**Abstract:** The naturally occurring alkaloid Huperzine A (HupA) is an acetylcholinesterase (AChE) inhibitor that has been used for centuries as a Chinese folk medicine in the context of its source plant *Huperzia Serrata*. The potency and relative safety of HupA rendered it a promising drug for the ameliorative treatment of Alzheimer's disease (AD) vis-à-vis the "cholinergic hypothesis" that attributes the cognitive decrements associated with AD to acetylcholine deficiency in the brain. However, recent evidence supports a neuroprotective role for HupA, suggesting that it could act as more than a mere palliative. Biochemical and crystallographic studies of AChE revealed two potential binding sites in the active-site gorge of AChE, one of which, the "peripheral anionic site" at the mouth of the gorge, was implicated in promoting aggregation of the beta amyloid (A $\beta$ ) peptide responsible for the neurodegenerative process in AD. This feature of AChE facilitated the development of dual-site binding HupA-based bivalent ligands, in hopes of concomitantly increasing AChE inhibition potency by utilizing the "chelate effect", and protecting neurons from A $\beta$  toxicity. Crystal structures of AChE allowed detailed modeling and docking studies that were instrumental in enhancing the understanding of underlying principles of bivalent inhibitor-enzyme dynamics. This monograph reviews two categories of HupA-based bivalent ligands, in which HupA and HupA fragments serve as building blocks, with a focus on the recently solved crystallographic structures of *Torpedo californica* AChE in complex with such bifunctional agents. The advantages and drawbacks of such structured-based drug design, as well as species differences, are highlighted and discussed.

**Keywords:** Acetylcholinesterase; Alzheimer's disease; bivalent ligand; chelate effect; huperzine A; hupyridone; tacrine; E2020.

## INTRODUCTION

(-)-Huperzine A [(-)-HupA] is an enantiomeric lycodine alkaloid isolated from the club moss *Huperzia serrata* of the *Lycopodium* species (*Huperziaceae*) [1]. The plant *H. serrata* itself is a centuries-old Chinese folk medicine (known as *Qian Ceng Ta*), traditionally used for the treatment of various maladies. (-)-HupA has been identified as a potent, specific and reversible inhibitor of the enzyme acetylcholinesterase (EC 3.1.1.7, AChE), relative to butyrylcholinesterase (EC 3.1.1.8, BChE). The extensive studies on (-)-HupA as a lead compound for the development of more effective anti-AChE drugs for the treatment of Alzheimer's disease (AD) relative to those approved by the FDA, such as donepezil (E2020, Aricept®) [2-4], (-)-galanthamine (Reminyl®) [5] and rivastigmine (Exelon®) [6], have been attributed to its better penetration through the blood brain barrier, its higher oral bioavailability and its longer duration of AChE inhibitory action [7, 8]. Phase IV clinical trials conducted in China demonstrated that (-)-HupA induces significant improvement in the memory of elderly people with AD and vascular dementia, without any noticeable side effects [8], and it is currently in phase II trials in the United States [9]. It has also been considered for use as a protective agent against organophosphate nerve agent intoxication [10].

It should be noted, however, that (-)-HupA has been shown to serve as a neuroprotective agent against a variety

of insults and, at a molecular level, has been shown to serve as an NMDA receptor antagonist [8]. Thus, novel lead compounds, based on the (-)-HupA scaffold, may have a broad spectrum of pharmacological actions, and not serve merely as anticholinesterase (anti-ChE) agents.

AD is a neurological disorder characterized by a significant decrease in hippocampal and cortical levels of the neurotransmitter acetylcholine (ACh), leading to severe memory and learning deficits [11]. According to the "cholinergic hypothesis" [12], inhibition of AChE in the central nervous system can alleviate these deficits; indeed, all first-generation AD drugs are cholinesterase inhibitors (ChEIs), including the synthetic compounds tacrine (Cognex®) [13, 14], donepezil (Aricept®) [2-4] and rivastigmine (Exelon®) [6], and the alkaloids (-)-galanthamine (Reminyl®) [5] and (-)-HupA (see above).

It has long been known that AChE has an enhanced affinity for bifunctional inhibitors such as the *bis*-quaternary inhibitors, decamethonium (DECA) [15], BW284c51 [16] and ambenonium [17] (Fig. 1) [18]. It was postulated that this is due to the existence of two binding sites in the enzyme [15]. These sites bind to the bivalent ligands simultaneously, giving rise to what is known as the "chelate effect". This is a well-known thermodynamic phenomenon that is manifested as the enhanced stability of a complex formed from bi- or polyvalent ligands and their targets, compared to a similar complex formed from the monovalent counterparts. This enhanced stability is the result of a decrease in entropic penalty for binding a single large ligand versus two smaller

\*Address correspondence to this author at the Weizmann Institute of Science, Rehovot 76100, Israel; Tel: +972-8-9344531; Fax: +972-8-9344159; E-mail: joel.sussman@weizmann.ac.il

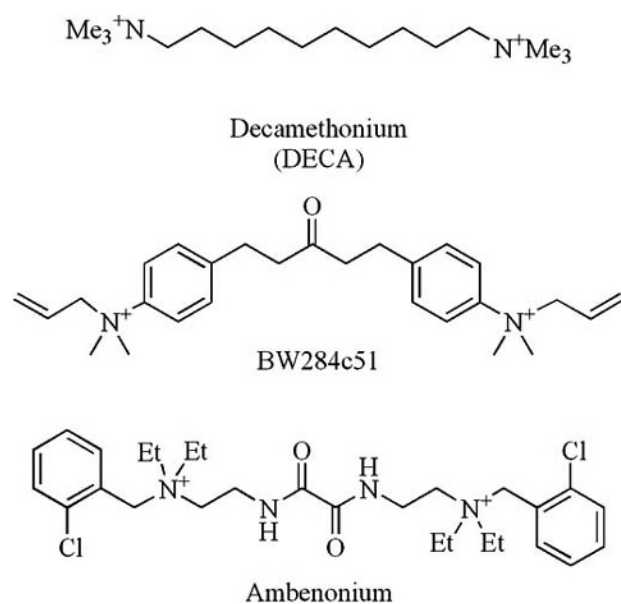


**Fig. (1).** Selected *bis*-quaternary bivalent AChE inhibitors.

ones, or the increase in the binding probability of a functional group in the ligand after the first one has bound [19]. The chelate effect is efficiently exploited by scientists in pursuit of stronger and more specific enzyme inhibitors that could serve as lead compounds for the development of potent drugs. Recent examples of such endeavors are the development of an HIV integrase inhibitor [20] and a potent bifunctional anticoagulant [21].

The crystal structure of AChE from the ray *Torpedo californica* (*TcAChE*) has provided invaluable insights into the catalytic mechanism of this remarkable enzyme [22]. A deep narrow gorge lined with aromatic residues penetrates halfway through the quasi-globular structure of the enzyme. At the bottom of the gorge resides the catalytic triad responsible for hydrolyzing ACh, and two aromatic side chains, tryptophan and phenylalanine (W84 and F330 in the case of *TcAChE*), that constitute the so-called “catalytic anionic subsite” (CAS) and make cation- interactions with the quaternary ammonium group of ACh [23, 24]. The “peripheral anionic site” (PAS) [25], that is responsible for the enhanced binding of bisquaternary ligands, was shown to be located near the entrance to the active-site gorge, and also contains two aromatic side chains, those of Y70 and W279. Subsequent solution of the 3D structures of a large repertoire of complexes and conjugates of AChE with a variety of inhibitors [26], in particular anti-AD drugs [27], provided a wealth of structural information which could be applied to the design of novel lead compounds. The crystal structure of the DECA/*TcAChE* complex clearly showed how the bisquaternary ligand orients along the active-site gorge, bridging the CAS and the PAS (Fig. 2) [28]. Thus, the structure of AChE and of complexes with gorge-spanning ligands, such as DECA and BW284c51 [29], provided a clear explanation for the chelate effect exhibited by dual-binding inhibitors. A large body of kinetic studies, utilizing site-directed mutagenesis, supports these structural assignments [30].

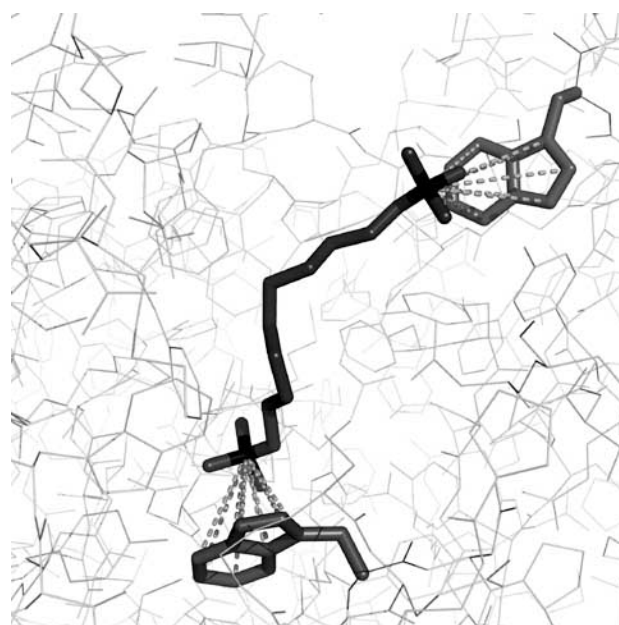


**Fig. (2).** Crystal structure of the DECA/*TcAChE* complex (PDB ID 1ACL). Protein residues are rendered as grey lines. Ligand and side chains W84 (bottom), and W279 (top) are rendered as sticks. Protein-ligand interactions are shown as broken lines. This image and subsequent representations of crystal structures were all created using PyMol [31].

Solution of the crystal structure of the (–)-HupA/*TcAChE* complex revealed the key structural features involved in their interaction, and opened the way for structure-based drug design based on the (–)-HupA template (Fig. 3) [32]. *In silico* docking experiments implied that (–)-HupA might bind not only at the bottom of the gorge, but also to the PAS [33]. Evidence for the existence of two potential binding sites, and the availability of high-resolution structures, have prompted the rational design of blood-brain barrier penetrable dual-affinity ligands, with the prospects of augmented specificity and potency of inhibition. The first such success was reported in 1996 with the design of *bis*(7)-tacrine (Fig. 4) [18, 33], and its structure in complex with *TcAChE* has been recently published [34]. There is accumulating evidence that *bis*(7)-tacrine has neuroprotective qualities that do not involve AChE inhibition, such as attenuation of neuronal apoptosis induced by the  $\beta$ -amyloid (A $\beta$ ) peptide via regulation of L-type Ca<sup>2+</sup> channels [35, 36]. It is generally accepted that A $\beta$  is the agent responsible for the neurodegenerative process in AD [37]. In this context, it is important to note that evidence has been presented that AChE can enhance the rate of aggregation of A $\beta$ , and that the PAS is the site on the enzyme involved in this action [38–42]. Thus, in addition to the palliative effect achieved by increasing ACh levels in the brain, inhibition of AChE may prove to have a neuroprotective role and to actually retard the progress of AD. It should also be noted that there is evidence that AChE plays ‘non-classical’ roles, in addition to its role in terminating transmission at cholinergic synapses [43], e.g. serving as an adhesion protein [44]. Thus, again, anti-ChE agents may have additional biological actions.

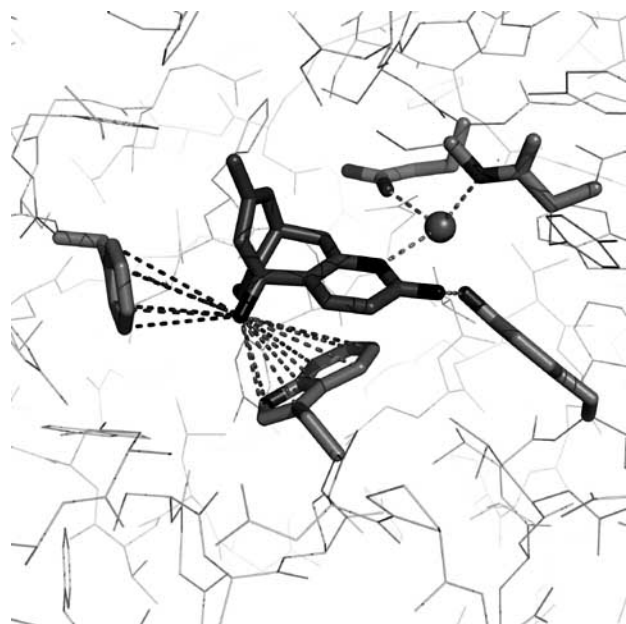


**Fig. (3).** Crystal structure of (-)-HupA (dark grey) bound at the active-site of TcAChE (PDB ID 1VOT). Protein residues are rendered as grey lines. The ligand and selected side chains are rendered as sticks. A water molecule is displayed as a grey sphere. Protein-ligand interactions are shown as broken lines.

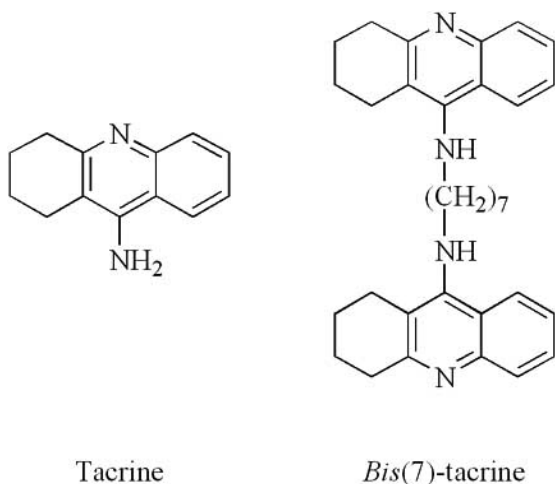


**Fig. (4).** Structures of tacrine (Cognex®) and bis(7)-tacrine.

In the following, two categories of huperzine dimers designed as lead compounds will be discussed: symmetric dimers, in which two HupA or HupA-derived pharmacophores are linked via an alkyl chain, and asymmetric ligands, in which the linker connects between HupA or a structurally related entity at one extremity and a different pharmacophore, e.g. tacrine, at the other extremity. Some of these ligands hold great promise as lead compounds; others have failed to show potential, but have taught us that much is yet to be explored to fully comprehend enzyme-inhibitor interplay within the active-site gorge of AChE.

### SYMMETRIC HUPERZINE LIGANDS

The most trivial species of a *bis*-huperzine ligand would be two (-)-HupA moieties connected via a tether (**1**), as shown in Fig. 5. Docking experiments suggested that a tether length of 7-12 carbons would be required for optimal dual-site binding of a *bis*-(-)-HupA dimer, **1**. Such dimers were synthesized and tested for their potency. Despite the coincidence of measured inhibition potencies with trends calculated from the docking studies, none of these bivalent ligands surpassed the monomer in their affinity [45]. Comparison of the crystal structures of (-)-HupA/TcAChE and (+)-HupA/TcAChE suggests an explanation for these findings [46]. Both (-)-HupA itself and (+)-HupA bind similarly at the bottom of the active-site gorge (Fig. 6), suggesting that one (-)-HupA subunit of the dimer would bind in a similar orientation to that of the monomer at the bottom of the gorge. In this binding orientation the pseudo-equatorial N5 that is fused to the linker in the (-)-HupA dimer points towards the bottom of the gorge, i.e. away from the PAS. One can envision that in this position, the bound (-)-HupA moiety will not easily accommodate an alkylene tether leading upwards towards the PAS; a longer linker may be required for optimum binding of both subunits to the enzyme. However, for the enantiomorph, (+)-HupA, the amino N5 atom is more favorably oriented; thus, a dimer composed of two (+)-HupA units might tolerate a shorter linker for optimal dual-site binding (Fig. 6).

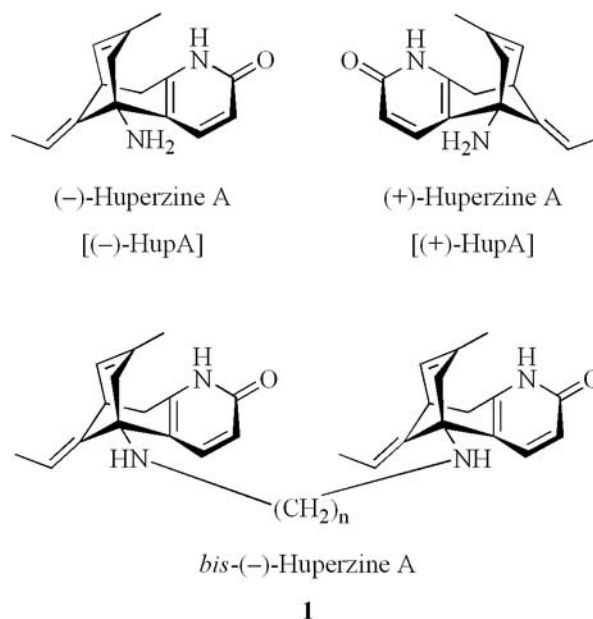


**Fig. (5).** Monovalent and bivalent huperzine A ligands.

In contrast to the previous example, where dimerization of a high affinity ligand failed to increase potency, the chelate effect can often produce a surprisingly high increase in binding affinity of bivalent inhibitors for AChE despite a low affinity of the corresponding monovalent pharmacophore for the PAS [18, 47]. Such is the case with another huperzine dimer, **2**, consisting of two (-)-Huperzine B [(-)-

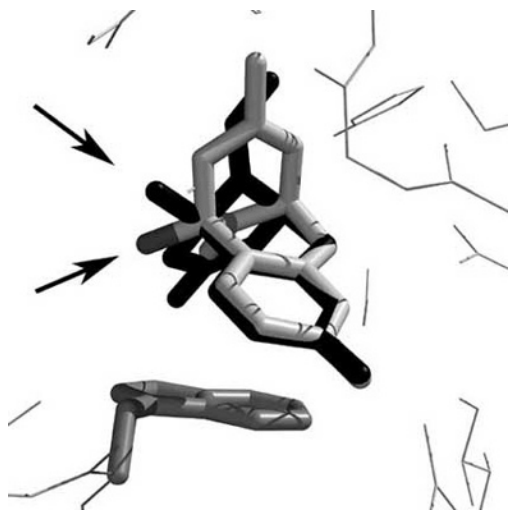


**Fig. (6).** Overlay structures of (-)-HupA (light grey) and (+)-HupA (dark grey) bound at the bottom of the active-site gorge of *TcAChE* (PDB codes 1VOT and 1GPK, respectively). Arrows point to the 5-amino group. Protein residues are rendered as grey lines. Ligands and the W84 side chain (bottom) are rendered as sticks.

HupB] moieties connected via a carbon-nitrogen chain (Fig. 7) [48]. (-)-HupB, which is very similar in structure to (-)-HupA, was also isolated from *H. serrata* [1]. The crystal structure of the (-)-HupB/*TcAChE* complex showed that (-)-HupB makes the same contacts with the enzyme as (-)-HupA, except that the ethylene-W84 interaction is absent in the (-)-HupB complex [46]. (-)-HupB has a weaker affinity for rat AChE (*rAChE*) than (-)-HupA, but dimerization enhanced potency by up to almost three orders of magnitude. In the optimal dimer (**2**) studied, the  $IC_{50}$  was improved from 19.3  $\mu$ M for the monomer to 4.9 nM for the dimer. Under the experimental conditions reported, this value was even lower than that for (-)-HupA (72.4 nM). Docking studies suggested that favorable interactions of the tether with several residues in the middle of the gorge contribute to the high potency of this dimer (Fig. 8). It is noteworthy that the optimal tether length, that of **2**, is 18 atoms. It is possible that the position of N5, oriented towards the bottom of the gorge in the crystal structure of the (-)-HupB/*TcAChE* complex, as was the case for the corresponding (-)-HupA complex, is the reason why a longer

tether is required. This supports the explanation for the apparent failure to increase affinity in the case of the (-)-HupA dimers studied (see above).

Another successful implementation of the chelate effect was the synthesis and evaluation of a (-)-HupA fragment, hupyridone (**3a,b**) (Fig. 9), and of corresponding bivalent derivatives. The dimers, (*S,S*)-(-)-**4a-c**, were designed on the basis of cumulative evidence that dimerization of weak or inactive fragments derived from (-)-HupA or from tacrine can produce potent ligands [47, 50, 51]. Compounds **3a,b** were initially synthesized with the rationale of preserving the key functionalities in (-)-HupA that had been observed to interact with residues at the active-site of the enzyme in the crystal structure. These are, specifically, the pyridone oxygen and the ring nitrogen, that are hydrogen-bonded to Y130 and to G117/Q199 (via a water molecule), and the 5-amino group which associates with W84 and F330 via cation- interactions (see Figs. 3 and 9) [32, 51]. The **3a,b** fragments, like their parent molecule, have a chiral center at position 5. The *N*-butyl-hupyridone control (**3c**) shows very weak inhibitory activity ( $IC_{50}$  of ~0.5 mM), but the enantiomeric dimers of the parent monomer (**3a**) are surprisingly potent. For example, the dimers (*S,S*)-(-)-**4b,c**, with corresponding 12- and 13-carbon tethers, both display  $IC_{50}$  values of 52 nM for *rAChE*. This four orders of magnitude increase in potency can be attributed in part to hydrophobic interactions of the carbon tether with the multiple aromatic residues lining the active-site gorge. In addition, docking studies performed for (*R*)- and (*S*)-**3b** showed that the binding orientation in the (*R*) configuration forces the 5-amino group to point towards the bottom of the gorge, which would not easily support a tether leading up the gorge to the PAS, thus rationalizing a 60-fold difference in affinity between the (*R,R*)- and (*S,S*)-enantiomers of **4b** [51].

In an attempt to understand the molecular determinants of the affinity of the **4** dimer series for AChE, and to compare them with those for the (-)-HupA/*TcAChE* complex, the crystal structures of both the (*S,S*)-(-)-**4a**/*TcAChE* and (*S,S*)-(-)-**4b**/*TcAChE* complexes were determined (Fig. 10) [52]. In these structures, both dimers bind in the expected manner, one **3a** monomer being positioned at the active-site, and the other at the PAS. At the active-site, the 5-amino moiety makes a cation- interaction with the aromatic rings of W84 and F330, and the aliphatic part of the **3a** entity makes hydrophobic interactions with

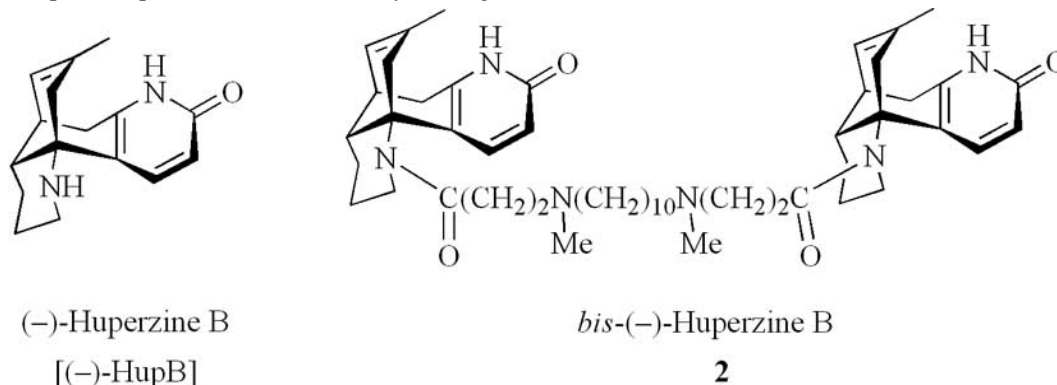


**Fig. (7).** Chemical structures of (-)-HupB and of a corresponding synthetic bivalent ligand.

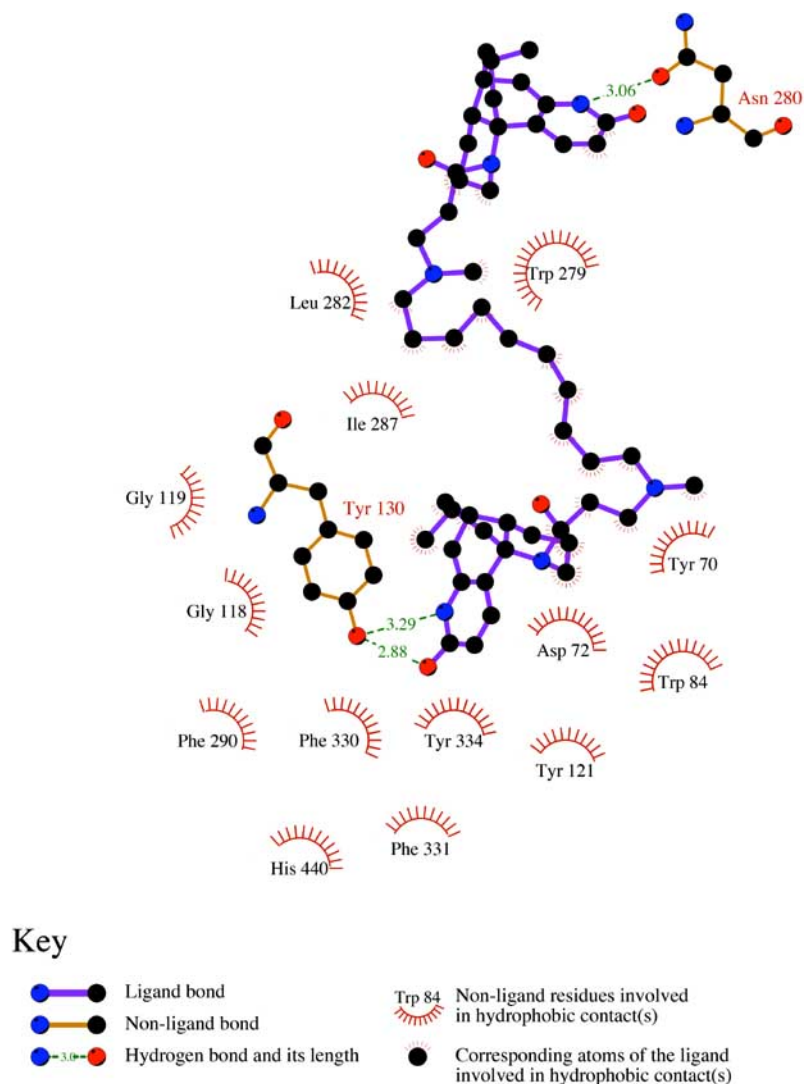


**Fig. (8).** Key interactions between the *bis*-(-)-HupB ligand, **2**, and amino acid residues in the active-site gorge of *TcAChE*, displayed using LIGPLOT [49]. Reproduced with permission from [48]. Copyright 2005 American Chemical Society".

W84 and F330. Similar interactions are made with W279 at the PAS. The pyridone oxygen and nitrogen make the same interactions at the bottom of the gorge as made by (-)-HupA. Obviously, interactions with the absent (-)-HupA ethylidene function are lacking, such as a  $\pi$ - $\pi$  interaction with the system of W84/F330, and the H-bond between the terminal methyl group of the ethylidene moiety and H440. A striking feature common to the structures of the *TcAChE* complexes with (-)-HupA, (+)-HupA, (-)-HupB and the (-)-**4a** and (-)-**4b** dimers, is a peptide bond-flip between G117 and G118 in the oxyanion hole at the active-site. This flip had been ascribed to repulsion between G117 O and the pyridone oxygen [46]. However, molecular dynamics studies simulating the binding and release of (-)-HupA from *TcAChE* indicate that the flip occurs even when the inhibitor is too distant to induce it directly, implying that a tendency to flip is an intrinsic property of this particular bond [53]. These simulations attribute a key role to D72 in drawing in and guiding (-)-HupA out of the active site, and stress the importance of "lubricating" water molecules in the active-

site gorge. The tether in the complexes of both the (-)-**4a** dimer and the (-)-**4b** dimer winds its way up the gorge, making what appear to be favorable hydrophobic interactions with the aromatic rings lining the gorge. At the PAS, the **3a** moiety is seen to fold back into the gorge, stabilized by hydrogen bonds of the pyridone oxygen and nitrogen with F288 and, via a water molecule, with R289 and S286.

The structures of the (-)-**4a,b**/*TcAChE* complexes make an important contribution to enhancing our understanding of the elements responsible for species-dependent differences in specificity and affinity of inhibitors. For *TcAChE*, the shorter 10-carbon tethered inhibitor binds better than its longer 12-carbon homologue, the  $IC_{50}$  values for (-)-**4a** and (-)-**4b** being 2.4 and 16 nM, respectively. However, for *rAChE*, the dimers reverse their affinities. The longer inhibitor is preferred, with the  $IC_{50}$  values being 151 and 52 nM for (-)-**4a** and (-)-**4b**, respectively. It is difficult to explain this reversal of inhibitory potency in terms of a

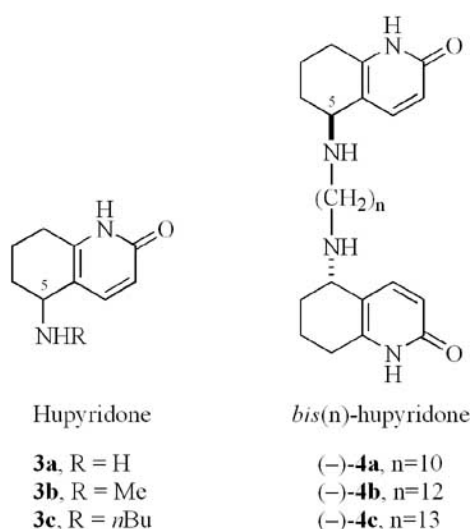


**Fig. (9).** Monovalent and bivalent hupridone ligands.

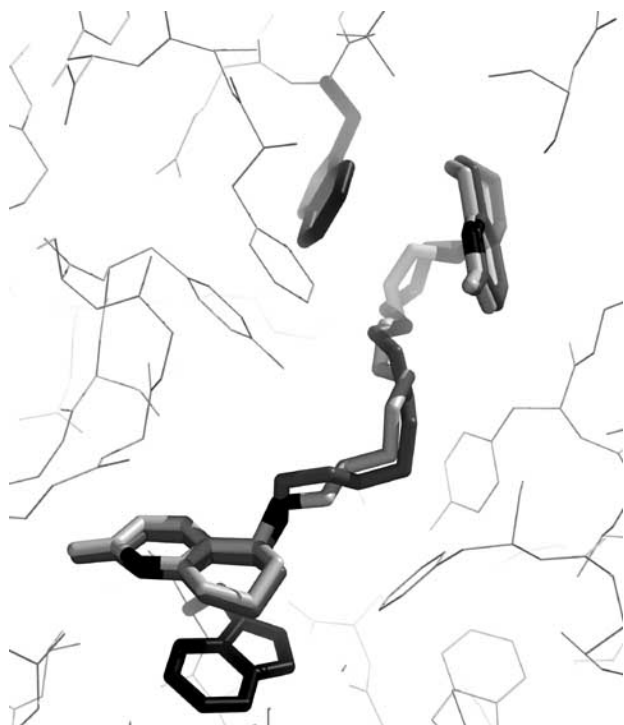


**Fig. (10).** Overlay structures of (*S,S*)-(-)-**4a** (light grey) and (*S,S*)-(-)-**4b** (dark grey) bound within the active-site gorge of TcAChE (PDB codes 1H22 and 1H23, respectively). Protein residues are rendered as grey lines. Ligands and side chains W84 (bottom) and W279 (top) are rendered as sticks.

reduced entropy loss, as it should favor the shorter linker in both cases, or likewise in terms of a reduced ligand-desolvation penalty, which should be consistent for the longer tether. The most plausible explanation is, therefore, that the preferences are inherent in different enzyme-inhibitor complementarities. Indeed, the mouse AChE (*m*AChE) structure [54], which is most likely very similar to that of *r*AChE, displays a narrowing of the gorge at its

bottom relative to that of TcAChE. In addition, the flexible F330 in TcAChE is homologous to Y337 in *m*AChE, which appears to be restricted in motion by H-bonding to Y341 via its hydroxyl, and is proposed by molecular modeling [55] to make a H-bond with the amino group of (-)-HupA. This may explain the enhanced affinity of (-)-HupA for mammalian AChE relative to TcAChE [52]. The rigidity of Y337 in mammalian AChE, relative to the flexibility of F330 in TcAChE, may force the linker in **4a/4b** to take a path in the mammalian enzymes different from the one observed in the TcAChE crystal structure, as is the case for DECA in *m*AChE vs TcAChE [54], resulting in the observed switch in dimer potencies between species (Fig. 11). The contributions of these subtle differences in structure to the differences

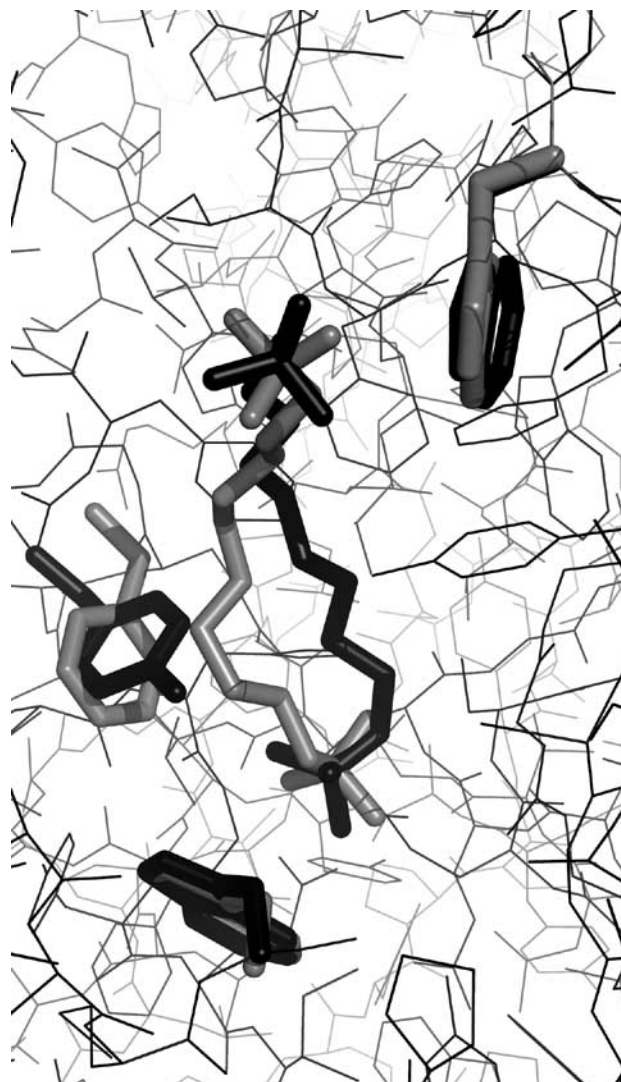


**Fig. (11).** Superimposition of the structures of the DECA/TcAChE complex (light grey) (PDB codes 1ACL) and the DECA/*m*AChE complex (dark grey) (PDB code 1MAA), showing the markedly different linker trajectories. Protein residues are rendered as thin lines. Ligands and selected side chains W84 (bottom), F330 (middle left) and W279 (top) are rendered as sticks; TcAChE residue numbering corresponds to residues W86, Y337 and W286, respectively, in *m*AChE.

observed in affinity demand more investigation. A clear understanding of their influence on, and interplay with, the thermodynamics of inhibitor binding is crucial for successful drug design.

### ASYMMETRIC HUPERZINE LIGANDS

Several bivalent ligands containing (-)-HupA or related pharmacophores linked to other groups have been reported. One such set of inhibitors are hybrids of a (-)-HupA-based pharmacophore and a fragment of E2020 [56]. E2020 (donepezil, Aricept®) is a potent, enantiomeric, benzylpiperidine-based AChE inhibitor approved for clinical treatment of AD in 1996, which is administered as a racemate, and extensively used for this purpose [57] (Fig. 12). The crystal structure of the E2020/*TcAChE* complex clearly shows its mode of binding [3]. (*R*)-E2020 spans the length of the gorge, with its proximal benzyl moiety stacked against W84, and its distal dimethoxyindanone group bound at the PAS (Fig. 13). The (*S*)-enantiomer of E2020 was not seen in the crystal structure, an observation suggestive of an inherent enantioselectivity of *TcAChE* for the (*R*)-enantiomer. Three HupA-E2020 hybrid compounds consisting of the benzylpiperidine moiety of E2020 linked to derivatives of (-)-HupA (**5a-c**) were reported (Fig. 12) [56]. These ligands were designed on the basis of docking studies with E2020 that resulted in an opposite orientation of the bound E2020 to the one seen in the solved crystal structure of the E2020/*TcAChE* complex, with the benzyl group being bound at the PAS, and the dimethoxyindanone moiety at the bottom of the gorge. Compound **5c** was a weak inhibitor ( $IC_{50}$  of 17.2  $\mu$ M) of *rAChE*, while the other two hybrids showed no significant inhibition. No reference to the stereochemistry of the compounds, nor any rationale for the selected modifications of the (-)-HupA-derived pharmacophores were provided, and it is possible that they were not tolerated by the enzyme.

(-)-Huperzine-tacrine hybrid ligands were designed with the objective of inhibiting both human AChE and BChE (*hAChE* and *hBChE*, respectively) [58]. BChE is widely distributed in vertebrate tissues, and in the brain it appears to be mostly of glial origin, while AChE is mostly of neuronal origin [59]. Despite its wide distribution, the physiological function of BChE is still uncertain [60]. An experiment conducted with knockout mice lacking the two functional alleles of AChE provided a truly striking observation. In spite of the complete absence of AChE from their bodies, and certain physiological features that bear resemblance to symptoms of inhibition of AChE, such as gastrointestinal hypomotility and a fine tremor, such mice are very much alive, can actually live up to several months, and have developed principal anatomical components of functional cholinergic pathways without any evident compensatory increase in the distribution of BChE [59, 61]. These remarkable results argue that BChE plays a constitutive role in hydrolyzing ACh in the mouse brain, since otherwise, the mice would have died from excessive cholinergic stimulation. Thus, by projection onto humans, BChE should be considered an important target, together with AChE, in the treatment of AD [60]. Molecular modeling studies based on the crystallographic structure of *hAChE* (PDB code 1B41) and a homology model of *hBChE* (PDB code 1EHO, based on *TcAChE*) assisted in the identification of a putative mid-gorge binding site in *hAChE* consisting of Y72/D74, and in *hBChE* consisting of N68/D70 [62]. These binding sites were targeted in the design of three bivalent inhibitors in which tacrine was connected, via a 7-carbon tether, to a (-)-HupA-derived pharmacophore (**6a-c**) (Fig. 14) [58]. Docking experiments done with the three inhibitors on *hAChE* suggest that the favorable binding orientations of both **6a** and **6b** position the tacrine group for a  $\pi$ -stacking interaction against W286 at the PAS, while the bicyclic

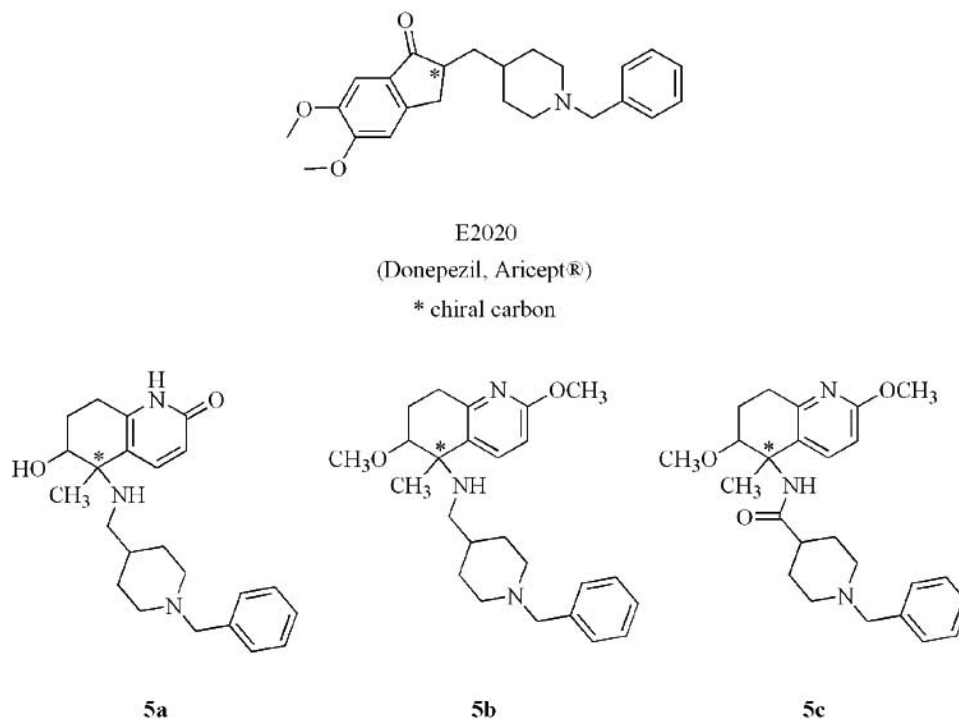
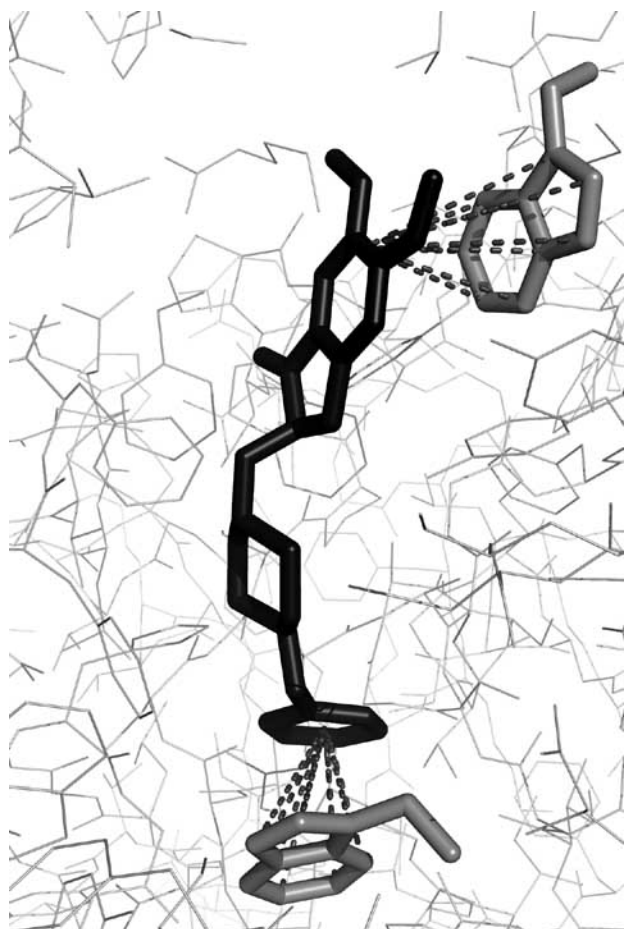


Fig. (12). Structures of E2020 and of HupA-E2020 hybrids.



**Fig. (13).** Complex of E2020 (dark grey) with *TcAChE* (PDB ID 1EVE). Protein residues are rendered as grey lines. The ligand and the side chains of W84 (bottom) and W279 (top) are rendered as sticks. Protein-ligand interactions are shown as broken lines.

group binds at the bottom of the gorge close to W86 (homologous to W84 in *TcAChE*). However, for the more potent inhibitor **6c**, the proposed binding orientation to *hAChE* is the opposite to that predicted for **6a** and **6b**; the tacrine moiety of **6c** is stacked against W86 at the CAS, as seen in a number of crystal structures of complexes of tacrine and tacrine-based inhibitors with *TcAChE* and *mAChE* (see for example Lit. [34, 63-66]), and the huperzine-fragment moiety interacts favorably with W286 at the PAS. In *hBChE*, the tacrine is stacked against W82 (homologous to W84 in *TcAChE*) for all three inhibitors, while the bicyclic moiety binds at the midpoint of the active-site gorge. The reported dissociation constants are of the same order of magnitude for all three inhibitors with respect to both enzymes. For *hAChE*, the inhibitors have significantly lower dissociation constants than tacrine, and with regard to *hBChE* they all display higher binding affinity than ( $\pm$ )-HupA.

The design of a hupyrindone-tacrine hybrid inhibitor, **6d** (Fig. 14), was based on the observation that  $\pi$ , cation- and hydrophobic interactions contribute to ligand affinity for the PAS [67]. The optimal tether length was found to be 10 carbons, yielding an  $IC_{50}$  of 8.8 nM for *rAChE*, i.e. 10- and 20-fold more potent than ( $\pm$ )-HupA and tacrine, respectively [68]. In an attempt to understand the mode of binding of this hybrid dimer, the structure of the **6d**/*TcAChE* complex was recently solved in both trigonal and orthorhombic crystal forms, after soaking the enzyme crystals with a racemic mixture of **6d** [64]. In both crystal forms, the tacrine moiety was seen to be bound at the active-site, sandwiched between W84 and F330, with its acridine amine hydrogen bound to H440, and the linker-fused nitrogen bound to a system of three conserved water molecules. This active-site binding mode is practically identical to the binding mode of monomeric tacrine reported previously in the tacrine/*TcAChE* complex [63], and similar to the orientation in complexes of other tacrine-based bivalent ligands with *TcAChE* and *mAChE* [34, 65, 66]. The 10-carbon linker spans the gorge

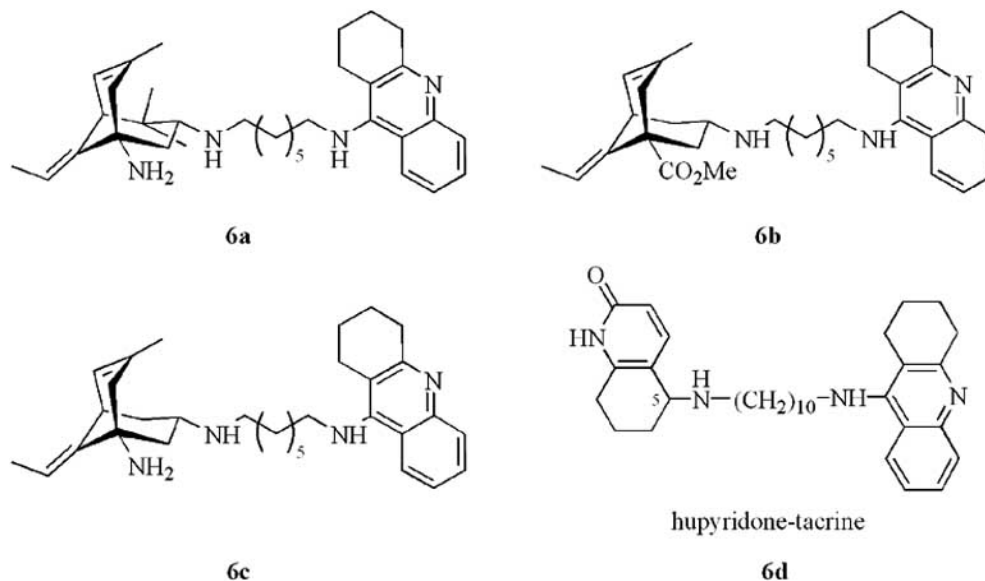


**Fig. (14).** Structures of ( $\pm$ )-huperzine-tacrine and hupyrindone-tacrine hybrids.

up to the PAS, where the secondary amino group linking it to the **3a** moiety makes a cation- interaction with W279. Surprisingly, in the trigonal structure solved initially, only the (*R*)-**3a** moiety of **6d** was visible, protruding outside the gorge, and aligned parallel to the gorge axis, with the pyridone oxygen and nitrogen bound to K11 and Q185 of a proximal, symmetry-related AChE molecule (Fig. 15). It was not clear from this structure whether the visible isomer in the gorge was selected out of the racemate due to an inherent preference of the enzyme arising out of steric constraints, or because of the crystal symmetry contacts of the **3a** subunit. This phenomenon merited further investigation, since both explanations bore interesting consequences: inherent preference of the enzyme for one enantiomer would imply potentially superior inhibition, whereas enantiomeric selection of

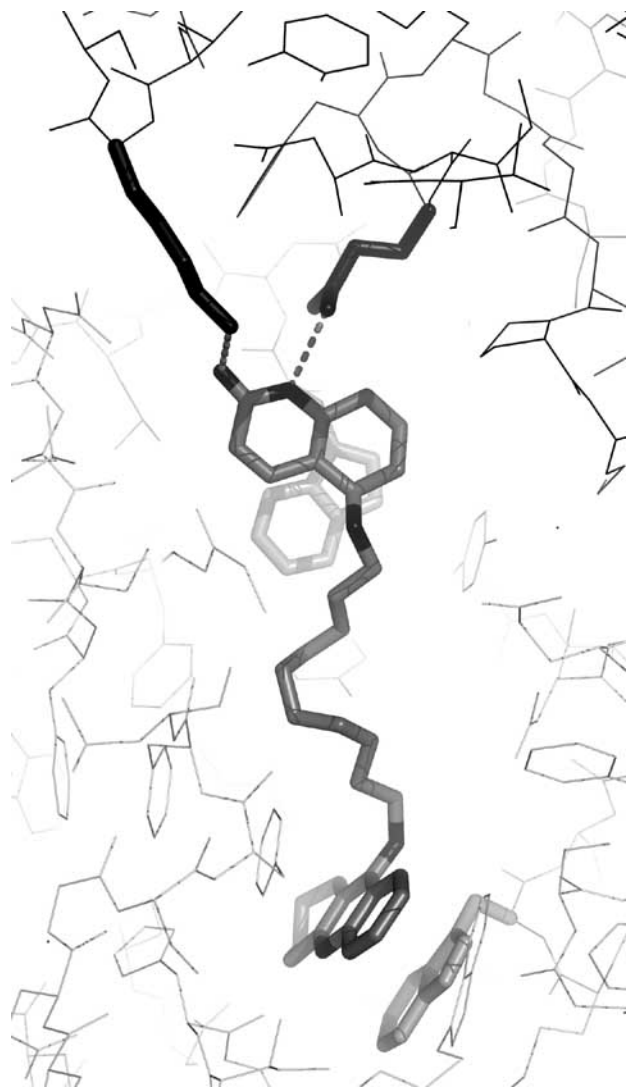


**Fig. 15.** Structure of (*R*)-**6d** (grey) bound within the active-site gorge in the trigonal *TcAChE* crystals (PDB ID 1ZGB). *TcAChE* residues in the parent molecule are rendered as light grey lines, symmetry-related *TcAChE* residues K\*11 and Q\*185 (top) are rendered as dark grey lines, and the side chains of W84 (bottom) and W279 (top) are rendered as sticks. Symmetry-related hydrogen bonds are shown as broken lines.

an inhibitor as an artifact arising as a consequence of crystal packing had never been reported. The issue was resolved by soaking orthorhombic *TcAChE* crystals with the racemate. For the orthorhombic crystals it had been established that the entrance to the gorge was remote from a symmetry-related molecule, *a priori* precluding symmetry-related interactions of the possibly protruding **3a** moiety of **6d** [69]. The orthorhombic **6d**/*TcAChE* crystal structure revealed both enantiomers bound at the active-site, i.e. approximately half of the molecules in the crystal bound the (*S*)-enantiomer (Fig. 16), while the other half bound the (*R*)-enantiomer. The (*S*)-**3a** moiety of **6d** at the PAS adopts a folded conformation essentially identical to the conformation of the (*S*)-**3a** moiety in the (–)-**4a**/*TcAChE* structure (see above), while the (*R*)-**3a** moiety of **6d** assumes a novel conformation, perpendicular

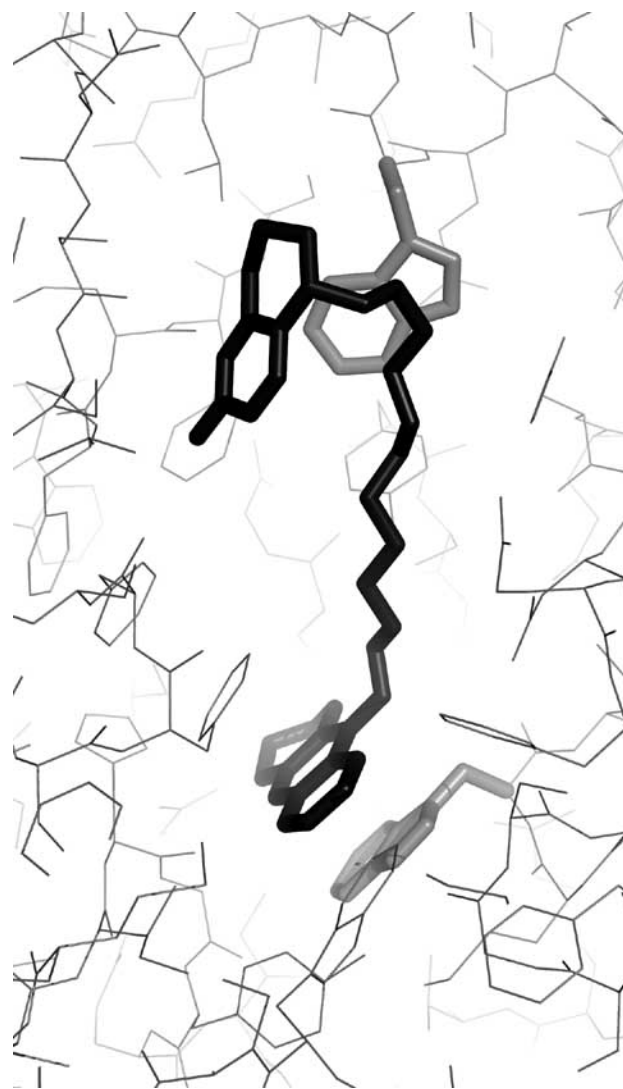


**Fig. 16.** Structure of (*S*)-**6d** (dark grey) bound within the active-site gorge in the orthorhombic *TcAChE* crystals (PDB ID 1ZGC). *TcAChE* residues are rendered as thin grey lines, and the side chains of W84 (bottom) and W279 (top) are rendered as sticks.

to the gorge axis. The unequivocal interpretation of these results is of an artifactual enantiomeric selectivity, due to crystal packing, which occurs in the trigonal crystals. Comparison of the orthorhombic (*S*)-**3a** vs. the trigonal (*R*)-**3a** mode of binding supplies a plausible explanation: the (*S*)-**3a** subunit makes only two H-bonds with the enzyme, while the (*R*) moiety makes three: two with the symmetry-related side chains of K11 and Q185, and one with S286 via a water molecule. Thus it is likely that in a competition between (*R*) and (*S*)-**6d** for binding to the enzyme in the trigonal crystal, the (*R*)-enantiomer has the upper hand due to favorable thermodynamics at the PAS. It is interesting to compare this phenomenon to the putative enantioselectivity reported for E2020 (see above).

## CONCLUSIONS AND FUTURE PROSPECTS

The application of quantitative structure-activity relationships (QSAR), molecular dynamics and X-ray crystallography in rational drug design, whether individually or in combination, has resulted in the discovery of numerous lead compounds that have served as starting points for obtaining drugs for the treatment of a broad repertoire of major diseases. The fact that, for AD, these approaches have already not only resulted in several approved drugs, but also in novel leads, is of especial importance, since the severe side effects often caused by ChEIs render the availability of several treatment regimens an imperative. Several fundamental features of the drug, the target enzyme, and the underlying principles of their interaction must be taken into consideration if better inhibitors are to be obtained:

- Crystal structures are snapshots of stable structures, and afford an excellent starting point for drug design; but thermodynamic considerations such as desolvation energies of the ligand, entropic penalties, and conformational destabilization of the protein, the ligand, or both, must be included in any simulation attempting to accurately predict the binding of a ligand.
- The solvent is ubiquitously involved in every aspect of the catalytic process and of inhibitor dynamics. Its role and contribution should, therefore, never be underestimated.
- The importance of the tether length in designing bivalent ligands which bind along the active-site gorge of AChE is threefold: i. It reduces entropy loss on binding; ii. It may enhance or diminish affinity by having its own beneficial or detrimental interactions with residues in the gorge; iii. It decreases the desolvation penalty of hydrophilic monomers by making them more hydrophobic.
- In certain cases, very high affinity of a monomer suggests strong interactions in a certain conformation or orientation. The introduction of a tether might impose conformational constraints that would interfere with optimal binding and, as a consequence, reduce affinity despite the chelate effect.
- The stereochemical configuration of a pharmacophore is critical not only for the monomeric inhibitor but also with regards to fusion position with the linker in bivalent AChE ligands.
- The crystalline state of the enzyme may generate artifacts with significant repercussions. Every structure should thus

be scrutinized and analyzed meticulously to avoid erroneous interpretations.

- Subtle differences in the dimensions of the active-site gorge, existence or absence of H-bond donors/acceptors, and conformational restriction of side chains leading to rigidity are all parameters that may explain variations in affinity for the same ligand from one species to another.

Overall, use of bivalent ligands has proven to be an extremely useful approach for improving the potency and specificity of AChE inhibitors, and crystal structures of AChE with various bivalent ligands have highlighted many of the underlying principles governing the mechanism of enzymatic catalysis and inhibition of AChE. A striking example for the effectiveness of this approach is the recent use of click chemistry, utilizing the active-site gorge of *Electrophorus electricus* AChE (*EeAChE*) as the 'reaction vessel' for generating a tacrine-phenylphenanthridinium bivalent inhibitor that exhibited 77 fM affinity for *TcAChE* (410 fM affinity for *mAChE*), and forced the enzyme into a unique conformation [65, 70]. Bifunctional derivatives have also been developed which successfully fulfill the dual tasks of inhibiting the catalytic activity of AChE and slowing the rate of A $\beta$  aggregation by the PAS [71, 72]. Other bifunctional gorge-spanning ligands have been developed which serve as dual inhibitors of AChE and monoamine oxidase [73], as dual anti-ChE and anti-inflammatory agents [74, 75], or as dual anti-ChE and protectants against reactive oxygen species [76]. As mentioned in the Introduction, (-)-HupA acts as a neuroprotectant against a variety of agents, whether as an *N*-methyl-D-aspartate (NMDA) receptor antagonist or by other mechanisms [8]. Thus bifunctional agents, in which (-)-HupA and (-)-HupA fragments serve as building blocks, may not only yield novel AChE inhibitors with improved pharmacological profiles for treatment of AD and other dementias, but may also find use as potent and specific drugs in a much broader context.

## ACKNOWLEDGMENTS

This project was supported by the Minerva Foundation, the Kalman and Ida Wolens Foundation, the Bruce Rosen Foundation, the Jean and Jula Goldwurm Memorial Foundation, the Divadol Foundation, the Benozzi Center for Neuroscience and the Kimmelman Center for Biomolecular Structure and Assembly, J.L.S. is the Pickman Professor of Structural Biology. We thank Prof. Paul R. Carlier (Department of Chemistry, Virginia Tech, Blacksburg, USA) for his support and encouragement.

## ABBREVIATIONS

A	=	-amyloid
ACh	=	Acetylcholine
AChE	=	Acetylcholinesterase (EC 3.1.1.7)
AD	=	Alzheimer's disease
Anti-ChE	=	Anticholinesterase
BChE	=	Butyrylcholinesterase (EC 3.1.1.8)
CAS	=	Catalytic anionic subsite
ChEI	=	Cholinesterase inhibitor

E2020	=	Donepezil
DECA	=	Decamethonium
EeAChE	=	<i>Electrophorus electricus</i> AChE
FDA	=	U.S. Food and Drug Administration
hAChE	=	Human AChE
hBChE	=	Human BChE
mAChE	=	Mouse AChE
NMDA	=	<i>N</i> -Methyl-D-aspartate
PAS	=	Peripheral anionic site
PDB	=	Protein Data Bank
QSAR	=	Quantitative structure-activity relationships
rAChE	=	Rat AChE
Tc	=	<i>Torpedo californica</i>

## REFERENCES

- Ma, X.; Gang, D. R. The Lycopodium alkaloids. *Nat. Prod. Rep.* **2004**, *21*, 752-772.
- Kawakami, Y.; Inoue, A.; Kawai, T.; Wakita, M.; Sugimoto, H.; Hopfinger, A. J. The rationale for E2020 as a potent acetylcholinesterase inhibitor. *Bioorg. Med. Chem. Lett.* **1996**, *4*, 1429-1446.
- Kryger, G.; Silman, I.; Sussman, J. L. Structure of acetylcholinesterase complexed with E2020 (Aricept): implications for the design of new anti-Alzheimer drugs. *Structure* **1999**, *7*, 297-307.
- Nightingale, S. L. Donepezil approved for treatment of Alzheimer's disease. *JAMA* **1997**, *277*, 10.
- Greenblatt, H. M.; Kryger, G.; Lewis, T.; Silman, I.; Sussman, J. L. Structure of acetylcholinesterase complexed with (-)-galanthamine at 2.3Å resolution. *FEBS Lett.* **1999**, *463*, 321-326.
- Bar-On, P.; Millard, C. B.; Harel, M.; Dvir, H.; Enz, A.; Sussman, J. L.; Silman, I. Kinetic and structural studies on the interaction of cholinesterases with the anti-Alzheimer drug rivastigmine. *Biochemistry* **2002**, *41*, 3555-3564.
- Bai, D. L.; Tang, X. C.; He, X. C. Huperzine A, a potential therapeutic agent for treatment of Alzheimer's disease. *Curr. Med. Chem.* **2000**, *7*, 355-374.
- Wang, R.; Yan, H.; Tang, X. C. Progress in studies of huperzine A, a natural cholinesterase inhibitor from Chinese herbal medicine. *Acta Pharmacol. Sin.* **2006**, *27*, 1-26.
- <http://www.clinicaltrials.gov/show/NCT00083590>
- Gordon, R. K.; Haigh, J. R.; Garcia, G. E.; Feaster, S. R.; Riel, M. A.; Lenz, D. E.; Aisen, P. S.; Doctor, B. P. Oral administration of pyridostigmine bromide and huperzine A protects human whole blood cholinesterases from ex vivo exposure to soman. *Chem. Biol. Interact.* **2005**, *157-158*, 239-246.
- DeKosky, S. T.; Scheff, S. W. Synapse loss in frontal cortex biopsies in Alzheimer's disease: correlation with cognitive severity. *Ann. Neurol.* **1990**, *27*, 457-464.
- Bartus, R. T.; Dean, R. L. r.; Beer, B.; Lippa, A. S. The cholinergic hypothesis of geriatric memory dysfunction. *Science* **1982**, *217*, 408-414.
- Davis, K. L.; Powchik, P. Tacrine. *Lancet* **1995**, *345*, 625-630.
- Watkins, P. B.; Zimmerman, H. J.; Knapp, M. J.; Gracon, S. I.; Lewis, K. W. Hepatotoxic effects of tacrine administration in patients with Alzheimer's disease. *JAMA* **1994**, *271*, 992-998.
- Bergmann, F.; Wilson, I. B.; Nachmansohn, D. The inhibitory effect of stilbamidine, curare and related compounds and its relationship to the active groups of acetylcholine esterase. Action of stilbamidine upon nerve impulse conduction. *Biochim. Biophys. Acta* **1950**, *6*, 217-224.
- Austin, L.; Berry, W. K. Two selective inhibitors of cholinesterase. *Biochem. J.* **1953**, *54*, 695-700.
- Lands, A. M.; Hoppe, J. O.; Arnold, A.; Kirchner, F. K. An investigation of the structure-activity correlations within a series of ambenonium analogs. *J. Pharmacol. Exp. Ther.* **1958**, *123*, 121-127.
- Du, D. M.; Carlier, P. R. Development of bivalent acetylcholinesterase inhibitors as potential therapeutic drugs for Alzheimer's disease. *Curr. Pharm. Des.* **2004**, *10*, 3141-3156.
- Jencks, W. P. On the attribution and additivity of binding energies. *Proc. Natl. Acad. Sci. U.S.A.* **1981**, *78*, 4046-4050.
- Long, Y. Q.; Jiang, X. H.; Dayam, R.; Sanchez, T.; Shoemaker, R.; Sei, S.; Neamati, N. Rational design and synthesis of novel dimeric diketoacid-containing inhibitors of HIV-1 integrase: implication for binding to two metal ions on the active site of integrase. *J. Med. Chem.* **2004**, *47*, 2561-2573.
- Lee, G. F.; Lazarus, R. A.; Kelley, R. F. Potent bifunctional anticoagulants: Kunitz domain-tissue factor fusion proteins. *Biochemistry* **1997**, *36*, 5607-5611.
- Sussman, J. L.; Harel, M.; Frolow, F.; Oefner, C.; Goldman, A.; Tokor, L.; Silman, I. Atomic structure of acetylcholinesterase from *Torpedo californica*: a prototypic acetylcholine-binding protein. *Science* **1991**, *253*, 872-879.
- Dougherty, D. A. Cation- interactions in chemistry and biology: a new view of benzene, Phe, Tyr, and Trp. *Science* **1996**, *271*, 163-168.
- Sussman, J. L.; Silman, I. Acetylcholinesterase: structure and use as a model for specific cation-protein interactions. *Curr. Opin. Struct. Biol.* **1992**, *2*, 721-729.
- Changeux, J.-P. Responses of acetylcholinesterase from *Torpedo marmorata* to salts and curarizing drugs. *Mol. Pharmacol.* **1966**, *2*, 369-392.
- Silman, I.; Sussman, J. L. Structural studies on acetylcholinesterase. In *Cholinesterases and Cholinesterase Inhibitors*, Giacobini, E. Ed. Martin Dunitz: London, 2000; pp 9-25.
- Greenblatt, H. M.; Dvir, H.; Silman, I.; Sussman, J. L. Acetylcholinesterase: a multifaceted target for structure-based drug design of anticholinesterase agents for the treatment of Alzheimer's disease. *J. Mol. Neurosci.* **2003**, *20*, 369-383.
- Sussman, J. L.; Harel, M.; Silman, I. Three-dimensional structure of acetylcholinesterase and of its complexes with anticholinesterase drugs. *Chem. Biol. Interact.* **1993**, *87*, 187-197.
- Felder, C. E.; Harel, M.; Silman, I.; Sussman, J. L. Structure of a complex of the potent and specific inhibitor BW284C51 with *Torpedo californica* acetylcholinesterase. *Acta Crystallogr. D Biol. Crystallogr.* **2002**, *58*, 1765-1771.
- Taylor, P.; Radic, Z. The cholinesterases: from genes to proteins. *Annu. Rev. Pharmacol. Toxicol.* **1994**, *34*, 281-320.
- DeLano, W. L. *The PyMOL Molecular Graphics System*, 0.99; DeLano Scientific: San Carlos, CA, USA, 2002.
- Raves, M. L.; Harel, M.; Pang, Y. P.; Silman, I.; Kozikowski, A. P.; Sussman, J. L. Structure of acetylcholinesterase complexed with the nootropic alkaloid, (-)-huperzine A. *Nat. Struct. Biol.* **1997**, *4*, 57-63.
- Pang, Y. P.; Kozikowski, A. P. Prediction of the binding sites of huperzine A in acetylcholinesterase by docking studies. *J. Comput. Aided. Mol. Des.* **1994**, *8*, 669-681.
- Rydberg, E. H.; Brumshtein, B.; Greenblatt, H. M.; Wong, D. M.; Shaya, D.; Carlier, P. R.; Pang, Y.-P.; Silman, I.; Sussman, J. L. Complexes of alkylene-linked tacrine dimers with *Torpedo californica* acetylcholinesterase: Binding of bis(5)-tacrine produces a dramatic rearrangement in the active-site gorge. *J. Med. Chem.* **2006**, *49*, 5491-5500.
- Fu, H.; Li, W.; Lao, Y.; Luo, J.; Lee, N. T.; Kan, K. K.; Tsang, H. W.; Tsim, K. W.; Pang, Y.; Li, Z.; Chang, D. C.; Li, M.; Han, Y. Bis(7)-tacrine attenuates beta amyloid-induced neuronal apoptosis by regulating L-type calcium channels. *J. Neurochem.* **2006**, *98*, 1400-1410.
- Li, W.; Lee, N. T.; Fu, H.; Kan, K. K.; Pang, Y.; Li, M.; Tsim, K. W.; Li, X.; Han, Y. Neuroprotection via inhibition of nitric oxide synthase by bis(7)-tacrine. *Neuroreport* **2006**, *17*, 471-474.
- Hardy, J.; Selkoe, D. J. The amyloid hypothesis of Alzheimer's disease: progress and problems on the road to therapeutics. *Science* **2002**, *297*, 353-356.
- Alvarez, A.; Alarcon, R.; Opazo, C.; Campos, E. O.; Munoz, F. J.; Calderon, F. H.; Dajas, F.; Gentry, M. K.; Doctor, B. P.; De Mello, F. G.; Inestrosa, N. C. Stable complexes involving acetylcholinesterase and amyloid- peptide change the biochemical properties of the enzyme and increase the neurotoxicity of Alzheimer's fibrils. *J. Neurosci.* **1998**, *18*, 3213-3223.

- [39] Alvarez, A.; Opazo, C.; Alarcon, R.; Garrido, J.; Inestrosa, N. C. Acetylcholinesterase promotes the aggregation of amyloid-peptide fragments by forming a complex with the growing fibrils. *J. Mol. Biol.* **1997**, *272*, 348-361.
- [40] Inestrosa, N. C.; Alvarez, A.; Perez, C. A.; Moreno, R. D.; Vicente, M.; Linker, C.; Casanueva, O. I.; Soto, C.; Garrido, J. Acetylcholinesterase accelerates assembly of amyloid-peptides into Alzheimer's fibrils: possible role of the peripheral site of the enzyme. *Neuron* **1996**, *16*, 881-891.
- [41] De Ferrari, G. V.; Canales, M. A.; Shin, I.; Weiner, L. M.; Silman, I.; Inestrosa, N. C. A structural motif of acetylcholinesterase that promotes amyloid-peptide formation. *Biochemistry* **2001**, *40*, 10447-10457.
- [42] Bartolini, M.; Bertucci, C.; Cavrini, V.; Andrisano, V. Amyloid aggregation induced by human acetylcholinesterase: inhibition studies. *Biochem. Pharmacol.* **2003**, *65*, 407-416.
- [43] Silman, I.; Sussman, J. L. Acetylcholinesterase: 'classical' and 'non-classical' functions and pharmacology. *Curr. Opin. Pharmacol.* **2005**, *5*, 293-302.
- [44] Paraoanu, L. E.; Layer, P. G. Mouse acetylcholinesterase interacts in yeast with the extracellular matrix component laminin-1. *FEBS Lett.* **2004**, *576*, 161-164.
- [45] Jin, G.; Luo, X.; He, X.; Jiang, H.; Zhang, H.; Bai, D. Synthesis and docking studies of alkylene-linked dimers of (-)-huperzine A. *Arzneimittelforschung* **2003**, *53*, 753-757.
- [46] Dvir, H.; Jiang, H. L.; Wong, D. M.; Harel, M.; Chetrit, M.; He, X. C.; Jin, G. Y.; Yu, G. L.; Tang, X. C.; Silman, I.; Bai, D. L.; Sussman, J. L. X-ray structures of *Torpedo californica* acetylcholinesterase complexed with (+)-huperzine A and (-)-huperzine B: Structural evidence for an active site rearrangement. *Biochemistry* **2002**, *41*, 10810-10818.
- [47] Pang, Y. P.; Quiram, P.; Jelacic, T.; Hong, F.; Brimjojn, S. Highly potent, selective, and low cost bis-tetrahydroaminacrine inhibitors of acetylcholinesterase. Steps toward novel drugs for treating Alzheimer's disease. *J. Biol. Chem.* **1996**, *271*, 23646-23649.
- [48] Feng, S.; Wang, Z.; He, X.; Zheng, S.; Xia, Y.; Jiang, H.; Tang, X.; Bai, D. Bis-huperzine B: highly potent and selective acetylcholinesterase inhibitors. *J. Med. Chem.* **2005**, *48*, 655-657.
- [49] Wallace, A. C.; Laskowski, R. A.; Thornton, J. M. LIGPLOT: a program to generate schematic diagrams of protein-ligand interactions. *Protein Eng.* **1995**, *8*, 127-134.
- [50] Han, Y. F.; Li, C. P.; Chow, E.; Wang, H.; Pang, Y. P.; Carlier, P. R. Dual-site binding of bivalent 4-aminopyridine- and 4-aminoquinoline-based AChE inhibitors: contribution of the hydrophobic alkylene tether to monomer and dimer affinities. *Bioorg. Med. Chem. Lett.* **1999**, *7*, 2569-2575.
- [51] Carlier, P. R.; Du, D. M.; Han, Y. F.; Liu, J.; Perola, E.; Williams, I. D.; Pang, Y. P. Dimerization of an inactive fragment of huperzine A produces a drug with twice the potency of the natural product. *Angew. Chem. Int. Ed. Engl.* **2000**, *39*, 1775-1777.
- [52] Wong, D. M.; Greenblatt, H. M.; Dvir, H.; Carlier, P. R.; Han, Y. F.; Pang, Y. P.; Silman, I.; Sussman, J. L. Acetylcholinesterase complexed with bivalent ligands related to huperzine A: experimental evidence for species-dependent protein-ligand complementarity. *J. Am. Chem. Soc.* **2003**, *125*, 363-373.
- [53] Xu, Y.; Shen, J.; Luo, X.; Silman, I.; Sussman, J. L.; Chen, K.; Jiang, H. How does huperzine A enter and leave the binding gorge of acetylcholinesterase? Steered molecular dynamics simulations. *J. Am. Chem. Soc.* **2003**, *125*, 11340-11349.
- [54] Bourne, Y.; Taylor, P.; Bougis, P. E.; Marchot, P. Crystal structure of mouse acetylcholinesterase. A peripheral site-occluding loop in a tetrameric assembly. *J. Biol. Chem.* **1999**, *274*, 2963-2970.
- [55] Dvir, H.; Wong, D. M.; Harel, M.; Barril, X.; Orozco, M.; Luque, F. J.; Muñoz-Torrero, D.; Camps, P.; Rosenberry, T. L.; Silman, I.; Sussman, J. L. 3D structure of *Torpedo californica* acetylcholinesterase complexed with huprine X at 2.1 Å resolution: kinetic and molecular dynamic correlates. *Biochemistry* **2002**, *41*, 2970-2981.
- [56] Zeng, F.; Jiang, H.; Zhai, Y.; Zhang, H.; Chen, K.; Ji, R. Synthesis and acetylcholinesterase inhibitory activity of huperzine A-E2020 combined compound. *Bioorg. Med. Chem. Lett.* **1999**, *9*, 3279-3284.
- [57] Winblad, B.; Kilander, L.; Eriksson, S.; Minthon, L.; Batsman, S.; Wetterholm, A. L.; Jansson-Blixt, C.; Haglund, A. Donepezil in patients with severe Alzheimer's disease: double-blind, parallel-group, placebo-controlled study. *Lancet* **2006**, *367*, 1057-1065.
- [58] Gemma, S.; Gabellieri, E.; Huleatt, P.; Fattorusso, C.; Borriello, M.; Catalanotti, B.; Butini, S.; De Angelis, M.; Novellino, E.; Nacci, V.; Belinskaya, T.; Saxena, A.; Campiani, G. Discovery of huperzine A-tacrine hybrids as potent inhibitors of human cholinesterases targeting their midgorge recognition sites. *J. Med. Chem.* **2006**, *49*, 3421-3425.
- [59] Mesulam, M. M.; Guillozet, A.; Shaw, P.; Levey, A.; Duysen, E. G.; Lockridge, O. Acetylcholinesterase knockouts establish central cholinergic pathways and can use butyrylcholinesterase to hydrolyze acetylcholine. *Neuroscience* **2002**, *110*, 627-639.
- [60] Greig, N. H.; Utsuki, T.; Ingram, D. K.; Wang, Y.; Pepeu, G.; Scali, C.; Yu, Q. S.; Mamczarz, J.; Holloway, H. W.; Giordano, T.; Chen, D.; Furukawa, K.; Sambamurti, K.; Brossi, A.; Lahiri, D. K. Selective butyrylcholinesterase inhibition elevates brain acetylcholine, augments learning and lowers Alzheimer beta-amyloid peptide in rodent. *Proc. Natl. Acad. Sci. U.S.A.* **2005**, *102*, 17213-17218.
- [61] Radic, Z.; Taylor, P. Structure and function of cholinesterases. In *Toxicology of organophosphate and carbamate compounds*, Gupta, R. C. Ed. Elsevier Academic Press: Amsterdam, 2006; pp 161-186.
- [62] Savini, L.; Gaeta, A.; Fattorusso, C.; Catalanotti, B.; Campiani, G.; Chiasserini, L.; Pellerano, C.; Novellino, E.; McKissic, D.; Saxena, A. Specific targeting of acetylcholinesterase and butyrylcholinesterase recognition sites. Rational design of novel, selective, and highly potent cholinesterase inhibitors. *J. Med. Chem.* **2003**, *46*, 1-4.
- [63] Harel, M.; Schalk, I.; Ehret-Sabatier, L.; Bouet, F.; Goeldner, M.; Hirth, C.; Axelsen, P. H.; Silman, I.; Sussman, J. L. Quaternary ligand binding to aromatic residues in the active-site gorge of acetylcholinesterase. *Proc. Natl. Acad. Sci. U.S.A.* **1993**, *90*, 9031-9035.
- [64] Haviv, H.; Wong, D. M.; Greenblatt, H. M.; Carlier, P. R.; Pang, Y. P.; Silman, I.; Sussman, J. L. Crystal packing mediates enantioselective ligand recognition at the peripheral site of acetylcholinesterase. *J. Am. Chem. Soc.* **2005**, *127*, 11029-11036.
- [65] Bourne, Y.; Kolb, H. C.; Radic, Z.; Sharpless, K. B.; Taylor, P.; Marchot, P. Freeze-frame inhibitor captures acetylcholinesterase in a unique conformation. *Proc. Natl. Acad. Sci. U.S.A.* **2004**, *101*, 1449-1454.
- [66] Colletier, J. P.; Sanson, B.; Nachon, F.; Gabellieri, E.; Fattorusso, C.; Campiani, G.; Weik, M. Conformational flexibility in the peripheral site of *Torpedo californica* acetylcholinesterase revealed by the complex structure with a bifunctional inhibitor. *J. Am. Chem. Soc.* **2006**, *128*, 4526-4527.
- [67] Carlier, P. R.; Chow, E. S.; Han, Y.; Liu, J.; El Yazal, J.; Pang, Y. P. Heterodimeric tacrine-based acetylcholinesterase inhibitors: investigating ligand-peripheral site interactions. *J. Med. Chem.* **1999**, *42*, 4225-4231.
- [68] Carlier, P. R.; Du, D. M.; Han, Y.; Liu, J.; Pang, Y. P. Potent, easily synthesized huperzine A-tacrine hybrid acetylcholinesterase inhibitors. *Bioorg. Med. Chem. Lett.* **1999**, *9*, 2335-2338.
- [69] Greenblatt, H. M.; Guillou, C.; Guenard, D.; Argaman, A.; Botti, S.; Badet, B.; Thal, C.; Silman, I.; Sussman, J. L. The complex of a bivalent derivative of galanthamine with *Torpedo* acetylcholinesterase displays drastic deformation of the active-site gorge: implications for structure-based drug design. *J. Am. Chem. Soc.* **2004**, *126*, 15405-15411.
- [70] Lewis, W. G.; Green, L. G.; Grynszpan, F.; Radic, Z.; Carlier, P. R.; Taylor, P.; Finn, M. G.; Sharpless, K. B. Click chemistry in situ: acetylcholinesterase as a reaction vessel for the selective assembly of a femtomolar inhibitor from an array of building blocks. *Angew. Chem. Int. Ed. Engl.* **2002**, *41*, 1053-1057.
- [71] Castro, A.; Martinez, A. Peripheral and dual binding site acetylcholinesterase inhibitors: implications in treatment of Alzheimer's disease. *Mini Rev. Med. Chem.* **2001**, *1*, 267-272.
- [72] Piazzzi, L.; Rampa, A.; Bisi, A.; Gobbi, S.; Belluti, F.; Cavalli, A.; Bartolini, M.; Andrisano, V.; Valenti, P.; Recanatini, M. 3-(4-[[Benzyl(methyl)amino]methyl]phenyl)-6,7-dimethoxy-2H-2-chromenone (AP2238) inhibits both acetylcholinesterase and acetylcholinesterase-induced beta-amyloid aggregation: a dual function lead for Alzheimer's disease therapy. *J. Med. Chem.* **2003**, *46*, 2279-2282.
- [73] Sterling, J.; Herzig, Y.; Goren, T.; Finkelstein, N.; Lerner, D.; Goldenberg, W.; Miskolczy, I.; Molnar, S.; Rantal, F.; Tamas, T.; Toth, G.; Zagyva, A.; Zekany, A.; Finberg, J.; Lavian, G.; Gross, A.; Friedman, R.; Razin, M.; Huang, W.; Kraiss, B.; Chorev, M.;

- Youdim, M. B.; Weinstock, M. Novel dual inhibitors of AChE and MAO derived from hydroxy aminoindan and phenethylamine as potential treatment for Alzheimer's disease. *J. Med. Chem.* **2002**, *45*, 5260-5279.
- [74] Farias, G. G.; Godoy, J. A.; Vazquez, M. C.; Adani, R.; Meshulam, H.; Avila, J.; Amitai, G.; Inestrosa, N. C. The anti-inflammatory and cholinesterase inhibitor bifunctional compound IBU-PO protects from  $\beta$ -amyloid neurotoxicity by acting on Wnt signaling components. *Neurobiol. Dis.* **2005**, *18*, 176-183.
- [75] Amitai, G.; Adani, R.; Fishbein, E.; Meshulam, H.; Laish, I.; Dahir, S. Bifunctional compounds eliciting anti-inflammatory and anti-cholinesterase activity as potential treatment of nerve and blister chemical agents poisoning. *J. Appl. Toxicol.* **2006**, *26*, 81-87.
- [76] Rosini, M.; Andrisano, V.; Bartolini, M.; Bolognesi, M. L.; Hrelia, P.; Minarini, A.; Tarozzi, A.; Melchiorre, C. Rational approach to discover multipotent anti-Alzheimer drugs. *J. Med. Chem.* **2005**, *48*, 360-363.